CHAPTER - 4

*Transparent conducting Tin dioxide thin films Prepared by open air chemical vapour deposition(OACVD) technique

*4.1 INTRODUCTION

The simultaneous occurrence of high optical transparency (more than 80 %) in the visible region and high electrical conductivity (about 10^3 Ω^{-1} cm^{-1} or more) is not possible in an intrinsic stoichiometric material. Partial transparency and fairly good conductivity may be obtained in thin films of a variety of metals. The only way to obtain good transparent conductors is to create electron degeneracy in a wide band gap (more than 3 eV) oxide by controllably introducing non-stoichimetry and /or appropriate dopants. The most popular transparent coatings are fabricated from metal oxides, in particular the oxides of indium, tin and zinc.

Tin oxide thin films are known to have high mechanical and chemical stability, except for their interaction with oxygen atoms at high temperature. These films have high transmittance in the visible region and a high reflectivity in the infrared region. They also possess a high electrical d.c. conductivity and Hall mobility. Undoped tin oxide films are n-type degenerate semiconductor with a wide band gap (approximately 3.5 - 4 eV) [1-3], and a refractive index of approximately 1.9 [3]. However, the properties of tin dioxide depend crucially on their deviation from stoichiometry, on the nature and amount of impurities, and on the microstructure. All these properties depend on the deposition method and parameters, and on post-deposition processing.

*** Published in the "journal of Thin Solid Films" Vol. 307 (1998) P. 221-227.**

Owing to their high chemical and mechanical stabilities, transparent conductive tin dioxide are largely employed in electrochemistry as transparent electrodes [4, 5] or as substrates for electrodeposition [6] in solid state devices for photovoltaic and optoelectronic applications [7-9] or as spectrally selective coatings [10]. Apart from these applications transparent conducting tin oxide can also be used in thin film resistors, transparent heating element for aircraft and automobile windows, antistatic coatings for instrument windows, heat reflecting mirrors for glass windows and incandescent bulbs, antireflection coatings, liquid crystal display, electrochromic and ferroelectric photoconductor storage, semiconductor / insulator / semiconductor (SIS) heterojunctions, and protective and wear-resistant coatings for glass containers [11]. There is growing interest in newer applications of tin oxide and one of the most important uses is for the detection of toxic and explosive gases in air such as carbon monoxide and methane [12,13].

Tin oxide is a high bandgap semiconductor which is made conductive by n-type dopants which fall into two categories: (i) pentavalent metals such as antimony which substitute for tin atoms, and (ii) halogens such as fluorine or chlorine which replace oxygen. The choice of dopant can be guided by understanding that tin oxide is a fairly ionic compound for which the metal orbitals dominantly form the conduction band, while the oxygen orbitals make up most of the filled valence band. Substituting a metal for tin induces a large local perturbation in the conduction band, frequently scattering the electrons in the conduction band. This reduces the mobility of the electrons, which degrades the conductivity and transparency of the material. A halogen substituting for oxygen, however, mainly disturbs the filled valence band, and only slightly disturbs the electrons in the conduction band. Of the halogens, fluorine causes the least scattering, and fluorine doping leads to tin oxide films with the highest conductivity [11], because these films generally have higher mobilities (about 25 - 50 cm^2

V^{-1} S^{-1}) than undoped SnO_2 films. In either type of substitution, a positively charged scattering center is produced.

Tin dioxide films have been prepared by various techniques such as chemical vapour deposition [14-18], spray pyrolysis [19-23], vacuum evaporation [24], reactive rf sputtering [25-28], sol-gel method [29-32] and glow discharge [33]. In this chapter, Open Air Chemical Vapour Deposition (OACVD) technique has been employed for the preparation of undoped and doped tin dioxide thin films and to study their different properties.

4.2. DEPOSITION OF SnO_2 FILM BY CVD

In the last several years, the deposition techniques for SnO_2 have undergone many changes, mainly as a result of the work of international research groups led by Bube, Bunshah, Manifacier and Chopra [1,8,11]. Many sophisticated deposition techniques have been developed. The foremost characteristics of a Chemical Vapour Deposition (CVD) technique is that it involves a heterogeneous chemical reaction at the surface of a substrate without requiring vacuum as an essential condition for deposition. The chemical reaction in CVD may be activated by the application of light, heat, RF field, x-ray radiation, electrical arc, glow discharge, electron bombardment, or by catalytic activity of the substrate surface.

Metallic oxides are usually deposited by the vaporization of a suitable metal-bearing compound (which is volatile, thermally stable at a temperature sufficiently high to produce an adequate vapour pressure and thermally unstable at higher temperatures of deposition - criteria generally fulfilled by organometallic compounds) and its in situ oxidation with O_2 or H_2O [34]. Argon, O_2 or N_2, are generally used as carrier gases. Some heterogeneous reactions leading to the formation of SnO_2 are given below.

$$SnCl_4(g) + O_2(g) \rightarrow SnO_2(s) + Cl_2 \quad ---(4.1.)$$

$$(CH_3)_4Sn(g) + 8O_2(g) \rightarrow SnO_2(s) + 6H_2O(g) + 4CO_2(g) \quad ---(4.2.)$$

$$SnCl_4(g) + 2H_2O \rightarrow SnO_2(s) + 4HCl(g) \quad ---(4.3.)$$

The mechanism of film formation via the above reactions has been throughly examined by Ghoshtagore [35]. In all cases, the reaction of $SnCl_2$ or $(CH_3)_4Sn$ has been found to take place at the surface with an adsorbed oxygen atom or water molecule. The main control parameters in the process are gas flow and composition, substrate temperature and geometry of the deposition apparatus. The deposition rate depends mainly on the gas flow rate and substrate temperature. Typical rates are about 300-1000 A^o min^{-1}, although much higher rates have been also reported [37,38]. The substrate temperature is generally in the range 350 - 400° C. Higher temperatures favour better crystallinity [34,39] and larger grain size [34,39-40] resulting in higher mobilities [34]. The geometry of the deposition system is of the utmost importance, especially for large-scale applications. A maximum solar transmittance of about 85% - 95% with a minimum resistivity as low as about 7 X 10^{-5} Ω cm is achievable by the CVD method [14-18 & 34-36].

In a previous report, Karanjai et al. [41] had described an extremly simple and low-cost chemical vapour deposition method for tin dioxide films. In that method, the starting material was $SnCl_2.2H_2O$ crystal which were ground with water into a paste and the paste applied in the form of 4-5 mm wide band near, and parallel to the lower edge of a substrate positioned vertically. On heating in air the paste decomposes according to the following equation.

$$6SnCl_2 + H_2O \rightarrow 2SnCl_4 + 4Sn(OH)Cl \quad ---(4.4.)$$

$SnCl_4$, which is generated as one of the reaction products, rises upward due to convection and hydrolyses on the heated substrate to produce a tin dioxide film according to the equation.

$$SnCl_4 + 2H_2O = SnO_2 + 4HCl \quad \ldots\ldots\ldots\ldots (4.5)$$

Doping with antimony can be achieved by mixing requisite amount of $SbCl_3$ with $SnCl_2$ paste. Considering the simplicity of the method, films of reasonable good quality can be obtained.

This so called "paste - heat " method, however suffers from the following disadvantages: (i) the portion of the substrate where the $SnCl_2$ paste was applied must be subsequently cut away before the films can be used, (ii) because of the geometry of the arrangement, the films are non-uniform, being thickest near the paste - coated area and becoming thinner away from it, and (iii) non-planar substrates, as also those with small sizes cannot be used.

4.3. EXPERIMENTAL DETAILS

Open Air Chemical Vapour Deposition (OACVD) method is mainly based on the principle of Chemical Vapour Deposition technique and modification of the above "paste-heat" method [41], which employs the same principle, and maintains essentially the same simplicity, at the same time enabling one to obtain films free from the defects discussed above. Here, the reaction is activated by heat only. It does not require any specialized sophisticated experimental setup, and hence can be carried out in any laboratory. In OACVD method the films were obtained simply by passing $SnCl_4$ vapour using air current due to convection through a long tube on a heated substrate in atmospheric conditions. Using this method, preparation of undoped and doped (Sb, Mo & F) tin dioxide thin films have been prepared and their electrical and optical properties as well as surface morphology and crystal structure are studied.

In this method a 75 cm. long glass tube of internal diameter 5 cm. was placed vertically as shown in Figure 4.1. The tube was heated from outside in atmospheric condition by winding a heater coil on its outer surface over a length of 70

cm. The substrate was placed vertically in the central region of the tube. The starting material was taken in a conical flask placed at the bottom of the tube and heated separately. The temperature of the substrate was measured by a thermocouple placed close to it. The starting material was prepared by mixing crystals of $SnCl_2$, $2H_2O$ with a few drops of water along with any dopant material that might be added and was stirred mechanically to convert it to a paste.

In the film forming process, the substrate was initially heated to attain the desired temperature after which the $SnCl_2$ paste was heated. White fumes were given off by the paste and were seen to deposit SnO_2 films where they came into contact with the hot substrate.

Using this method, it is possible to deposit a number of films in a batch, by attaching them to a holder, which is placed in the central region of the tube. Usually both sides of the substrate are coated by this method, which is advantageous in some special cases [42], but it is also possible to coat one side only by masking the other side, or by fixing two substrates back to back. This method is especially advantageous for inaccessible surfaces and the inside surface of a tube, where one can obtain a coating quite easily, in contrast to rather complex arrangements required in usual CVD methods. The films were usually deposited over microglass slides (7.5 cm. x 2.5 cm.) and showed uniform interference colour over their entire area except at the edges. But uniform films could also be routinely obtained, if necessary, over a larger area of 40 cm. long by 4 cm. wide.

Undoped tin dioxide films of various thicknesses were prepared at substrate temperatures of 350° C, 400° C and 450° C. Soda glass microslides, mica and Al-sheet were used as substrates.

The films were doped with Antimony, Fluorine and Molybdenum by adding Antimony trichloride (15 mg for 1.5 at% Sb-doped), Ammonium fluoride (275

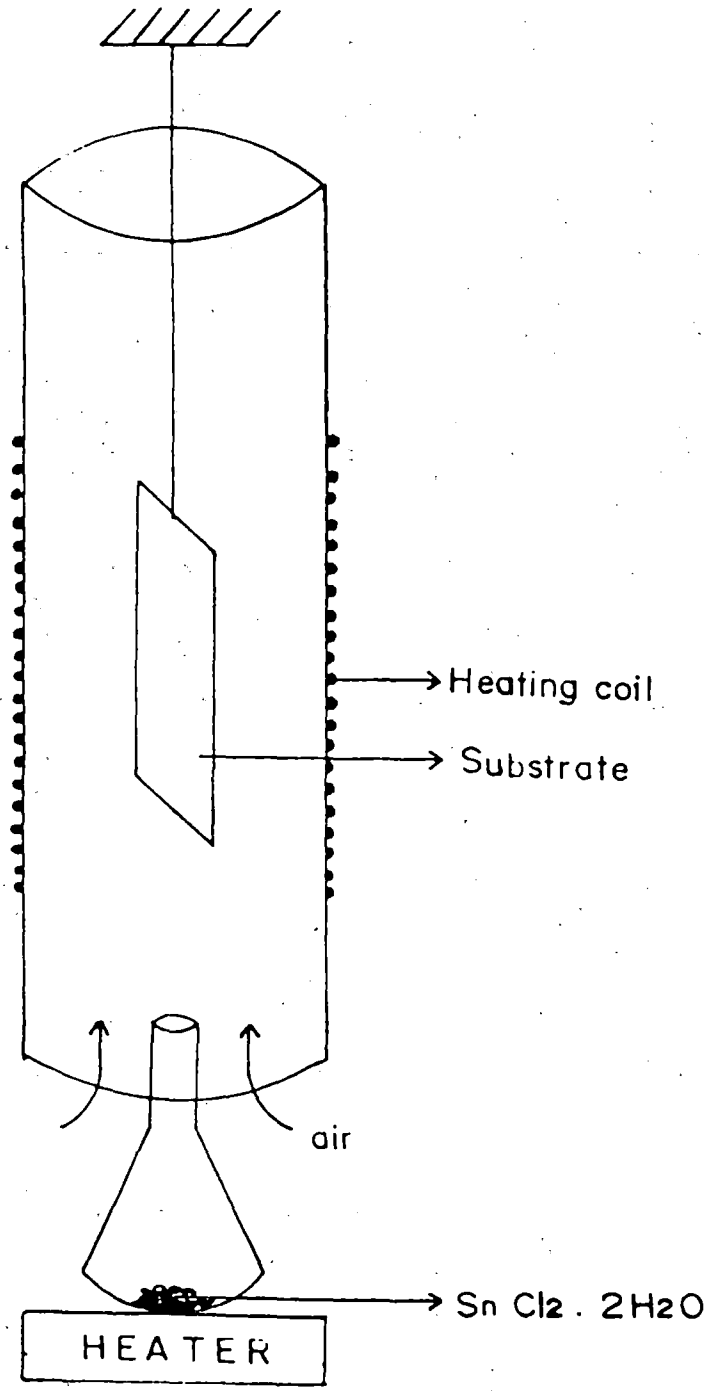

Figure 4.1. Experimental setup of Open Air Chemical Vapour Deposition (OACVD) method for deposition of thin films.

mg for 4.5 at% F-doped) and Ammonium molybdate (70 mg for 6 at% Mo-doped) respectively to the $SnCl_2.2H_2O$ (25 gm) starting material. Electronic grade materials were used for the preparation of these films. Characterization of the films was carried out by optical transmission and electrical conductivity measurments, X-ray diffractometry and scanning electron microscopy.

4.4.EXPERIMENTAL RESULTS

The films were smooth, highly uniform and resistant to peeling - off and acids, and also showed long term stability with respect to their optical, electrical and mechanical properties. They displayed characteristic interference colours. It was found that using this process a substrate temperature of 400° C was necessary to prepare films of the very high quality in terms of conductivity, optical transmission, uniformity and resistance to peeling - off and acids as well as environmental shocks.

4.4.1. X- ray diffractometric study

The undoped and doped tin dioxide films are polycrystalline and have a rutile structure with lattice parameters corresponding to those of bulk tin dioxide. Although the undoped tin dioxide films are randomly oriented, doping leads to orientation effects.

X-ray diffractometric studies were carried out on undoped and doped (Sb, Mo & F) SnO_2 films deposited at a substrate temperature of 400° C using Philips diffractometer (model PW 1390) with CuK_α radiation at 1.54 Å. Diffraction peaks for undoped SnO_2 films having two different thicknesses are shown in figure 4.2(a). Figure 4.2(b) shows the x-ray diffractograms of Sb and F-doped SnO_2 films. The crystal structure is in accordance with the usual tetragonal form of SnO_2 .

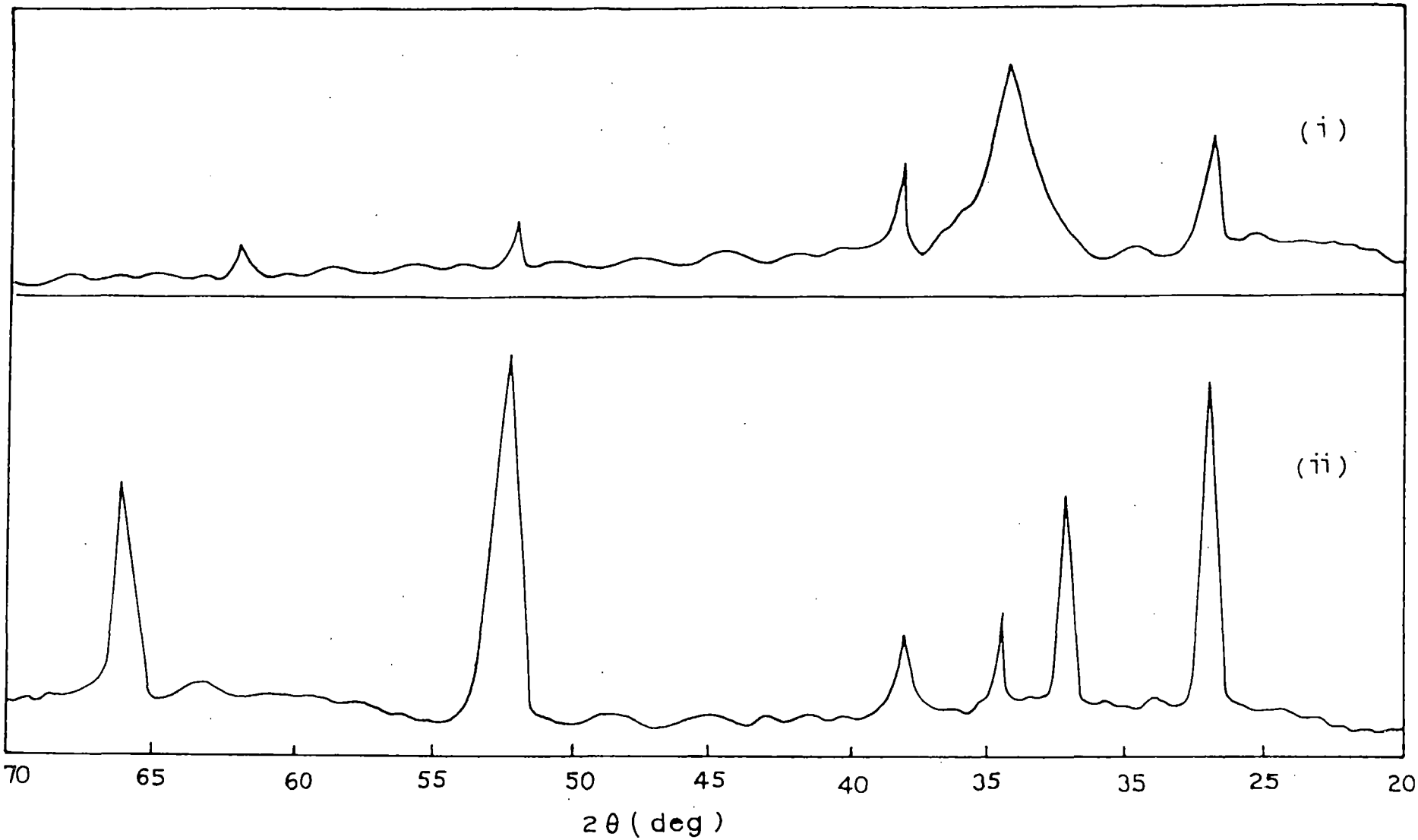

Figure 4.2. (a). X-ray diffractogram of undoped SnO_2 films of two different thickness (T_s = 400° C) (i) 0.6 μm (ii) 2.5 μm.

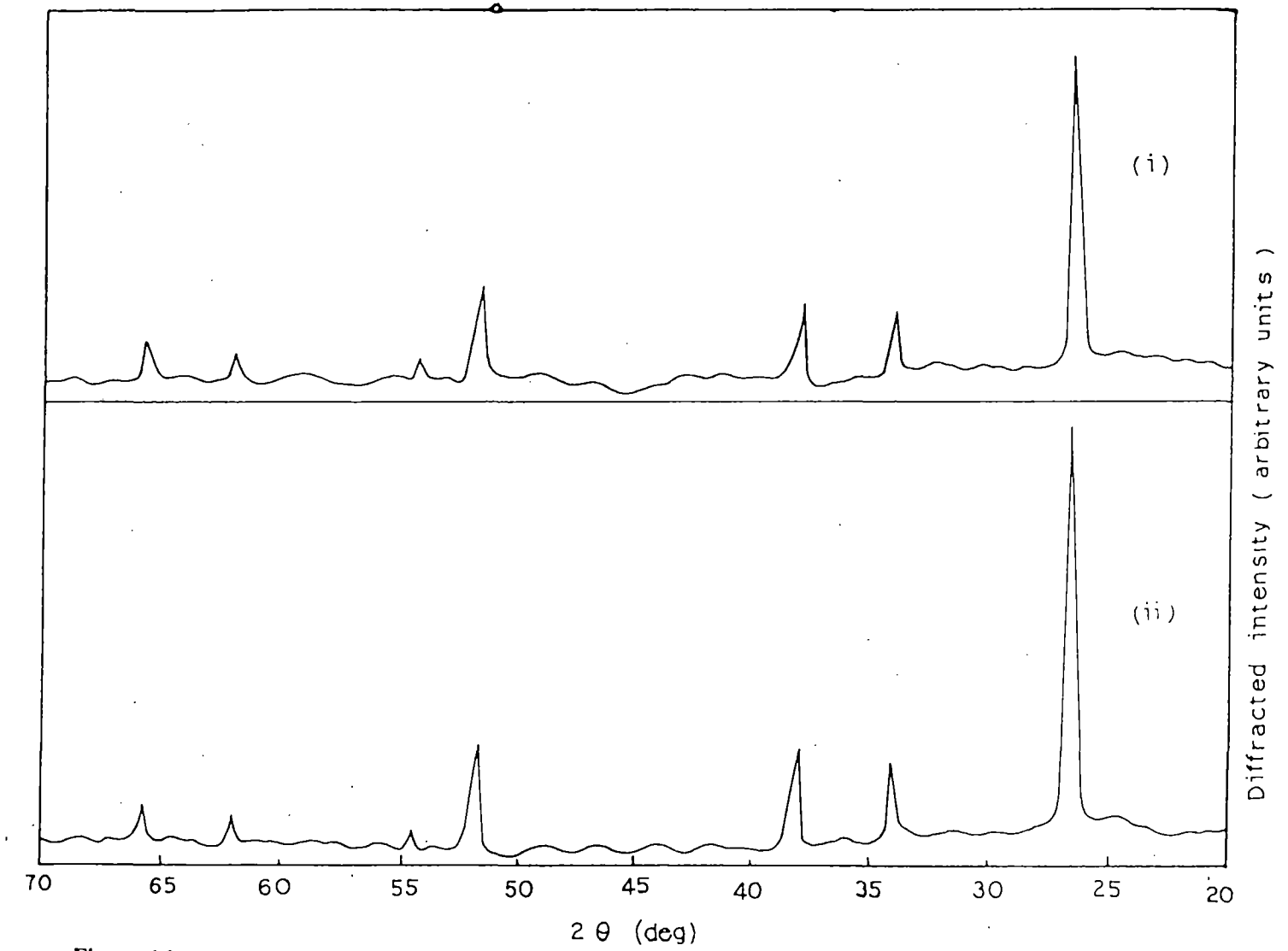

Figure 4.2.(b) X-ray diffractogram of doped SnO_2 films (T_s= 400° C). (i) 1.5 at% Sb-doped, (ii) 4.5 at% F-doped

It is clear from the XRD patterns that there is no amorphous background in the diffractograms of the deposited films. Moreover, none of the undoped films show any preferred orientation, while those doped with Sb and F shows preferred orientation along the (110) planes. Prominent peaks, their d-values and relative intensities (I/I_0) for a typical F-doped films are listed in Table - 4.1.

Table - 4.1. ***Prominent peak position (2θ values) of the X- ray diffraction peaks, corresponding d - values, relative intensities (I/I_0) and their identification for F - doped SnO_2 films.***

Observed Values			**Comparable values from ASTM data file**			
(2θ)	d-values(A^o)	(I/I_0)	(2θ)	d-values(A^o)	(I/I_0)	h k l
26.60	3.347	100	26.57	3.351	100	110
33.90	2.641	21	33.86	2.644	80	101
37.95	2.368	32	37.94	2.369	25	200
51.75	1.764	34	51.73	1.765	65	211
54.85	1.671	12	54.74	1.675	18	220
61.95	1.496	12	61.86	1.498	14	310
65.90	1.415	13	65.94	1.415	16	301

4.4.2. Surface Morphology

Surface morphology studies were carried out by HITACHI S-530 scanning electron microscopy. The scanning electron micrographs of these films indicated that the coarseness of the surface increases with increasing deposition temperature and dopant concentration. Surface topographies of undoped, 6 at% Mo-doped, 1.5 at% Sb-doped, and 4.5 at% F-doped SnO_2 films deposited at a substrate temperature of

400° C are shown in figure 4.3. It is observed that in all cases except that of Mo-doped films large size grains of ~ 1.7 μm are spread through out the film over a background of grain size ~ 0.6 μm. These large grains are observed to disappear when doped with Mo. The average grain size for Sb and F-doped films are found to be larger, while that for Mo-doped films are smaller compared to the undoped ones.

Films were also deposited on different substrates to investigate the substrate effect. Figure 4.4 shows the SEM micrographs of undoped SnO_2 films deposited on mica and aluminium sheet at a substrate temperature of 400° C. It is also evident from figure 4.4 that the grain size of the undoped SnO_2 films deposited on crystalline mica and aluminium substrate is larger than that deposited on glass substrates. Table 4.2 shows the grain size variation of the film deposited.

Table 4.2. *- Grain size variation of doped (on glass) and undoped (on different substrates) SnO_2 films [deposition temperature T_S = 400° C].*

Films	Substrate	Average grain size (μm)
SnO_2-undoped	glass	1.20
SnO_2:Sb	glass	4.00
SnO_2:Mo	glass	0.60
SnO_2:F	glass	4.75
SnO_2-undoped	mica	2.00
SnO_2-undoped	aluminium	1.50

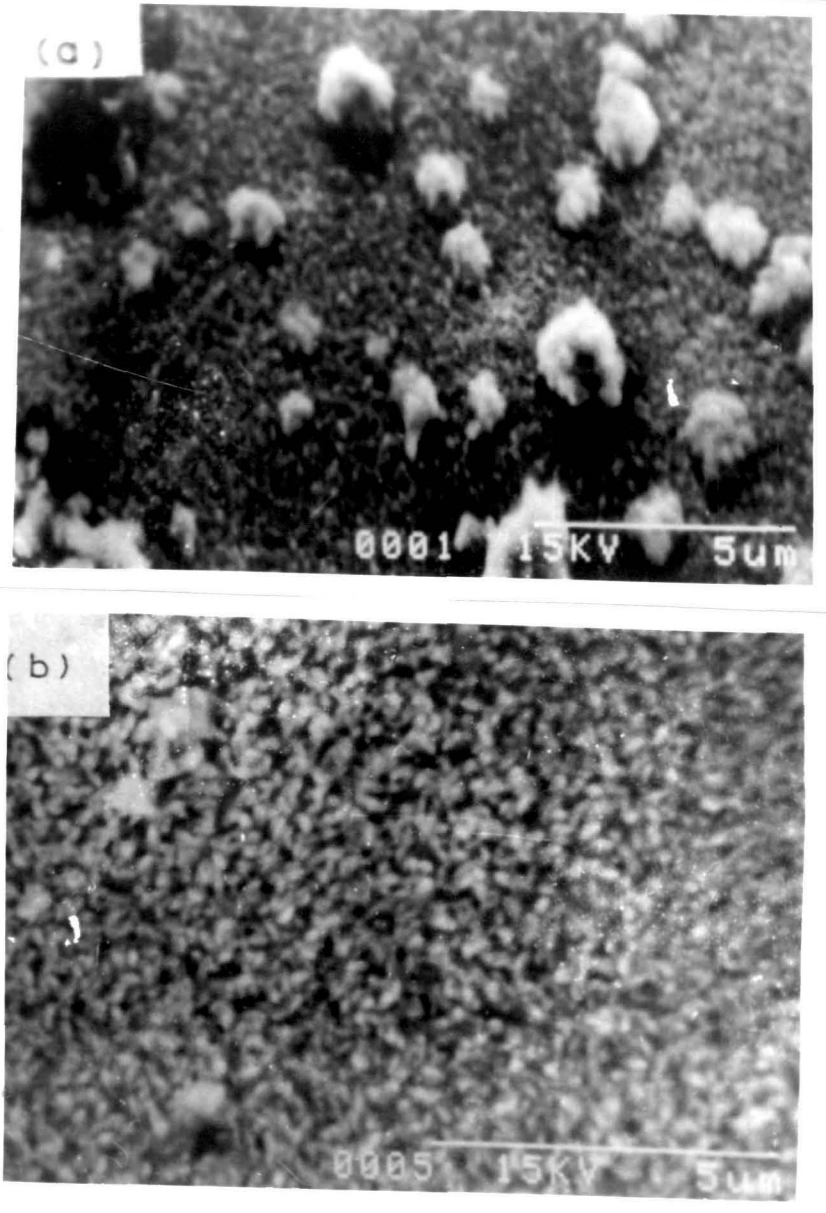

Figure 4.3. Scanning electron microscopes of undoped and doped SnO_2 thin films on glass substrate (T=400^0 C). (a) Undoped SnO_2; (b) SnO_2:Mo (6 at%).

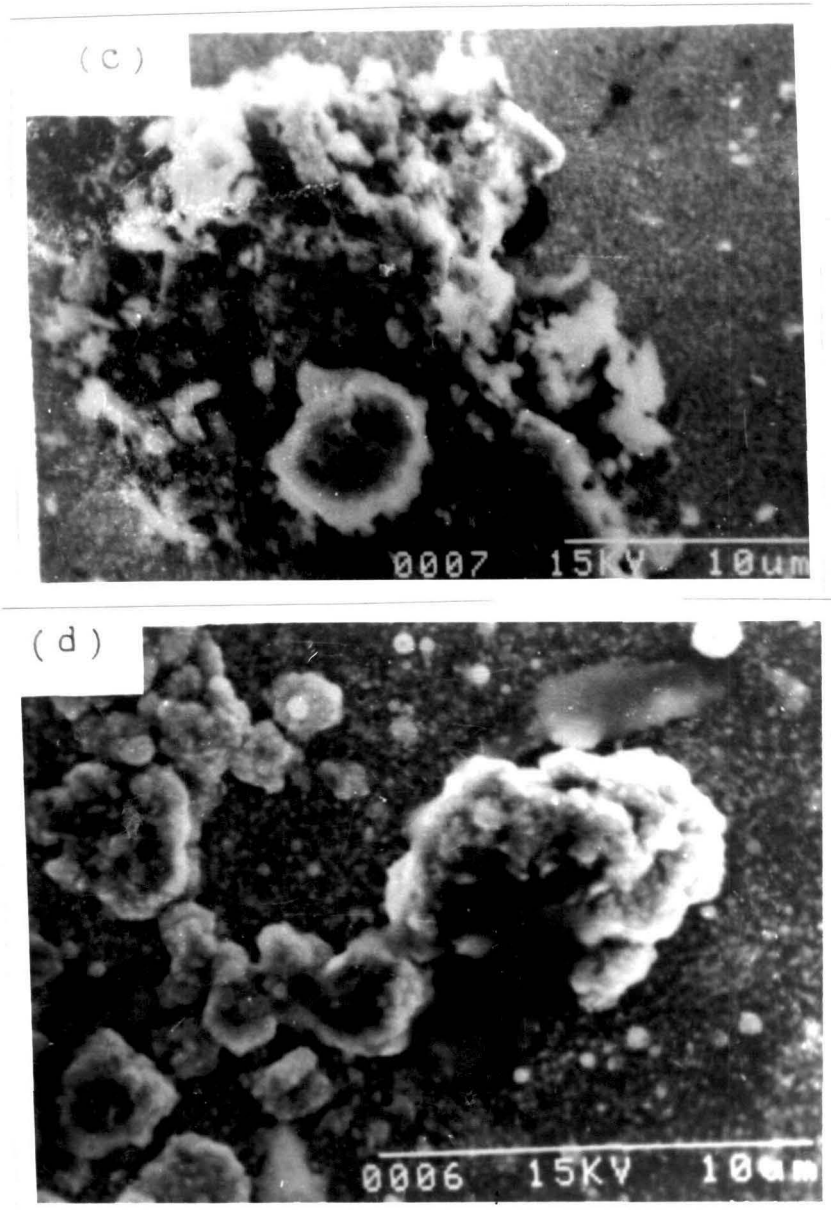

Figure 4.3. Scanning electron microscopes of doped SnO_2 thin films on glass substrate (T=400° C). (c)SnO_2:Sb (1.5 at%) (d) SnO_2:F (4.5 at%).

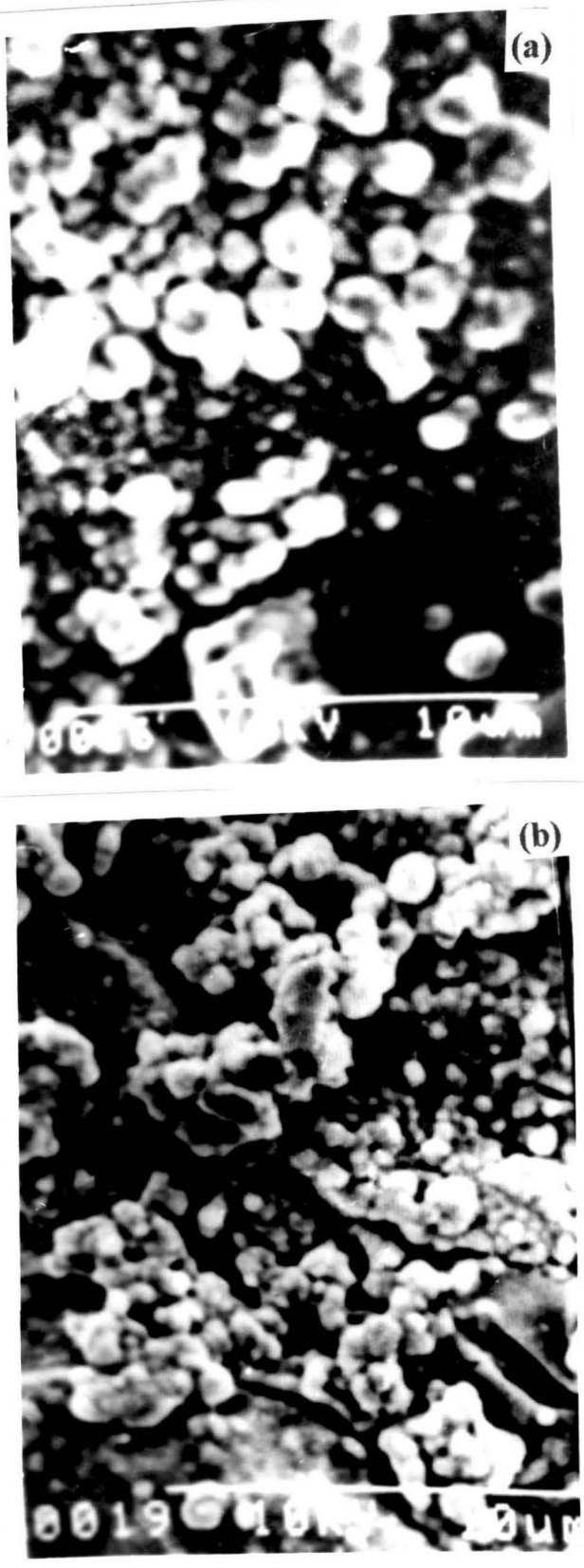

Figure 4.4. Scanning electron microscopes of SnO_2 thin films on different substrates (T=400^0 C) (a) mica (b) On aluminium sheet.

4.4.3. Electrical Properties

Results of detailed measurments of sheet resistance of the films as a function of thickness, temperature and dopant concentration are shown in Figures 4.5, 4.6 and 4.7 respectively. Films of various thickness were obtained by varying the amount of starting material, deposition time and substrate temperature. By observing the change in interference colours as a function of time the order of a particular colour could be known, and from the standard value of mean refractive index of SnO_2 (taken as 2.0 over the range 400 nm - 800 nm) the thickness could be estimated [43]. The sheet resistance of the films were measured by standard four-probe method.

Figure 4.5 shows the variation of sheet resistance with thickness of undoped films deposited at three substrate temperatures. It is evident from the curves that the room temperature resistivity of the undoped films decreases to its minimum value when deposited at a substrate temperature of 400° C but increases again when deposited at a higher substrate temperature of 450° C. This is due to the fact that, on increasing the substrate temperature from 350° C to 400° C, a better degree of crystallinity is achieved, leading to improved electronic, optical and structural properties [44-45]. It is also known that [21] both the carrier concentration and mobility increase with the increase of substrate temperature where mobility variation is larger than that of carrier concentration. Further increase in substrate temperature produces films of increased resistivity. This is due to the fact that in undoped SnO_2, conduction electrons arise from oxygen vacancies, and higher substrate temperature causes increased oxygen evolution from the substrate, leading to more nearly stoichiometric films [14,44]. The resistivity of the undoped films prepared at a substrate temperature of 400° C is estimated to be 4×10^{-3} Ω cm., which agrees well with the values reported earlier in the literature [44].

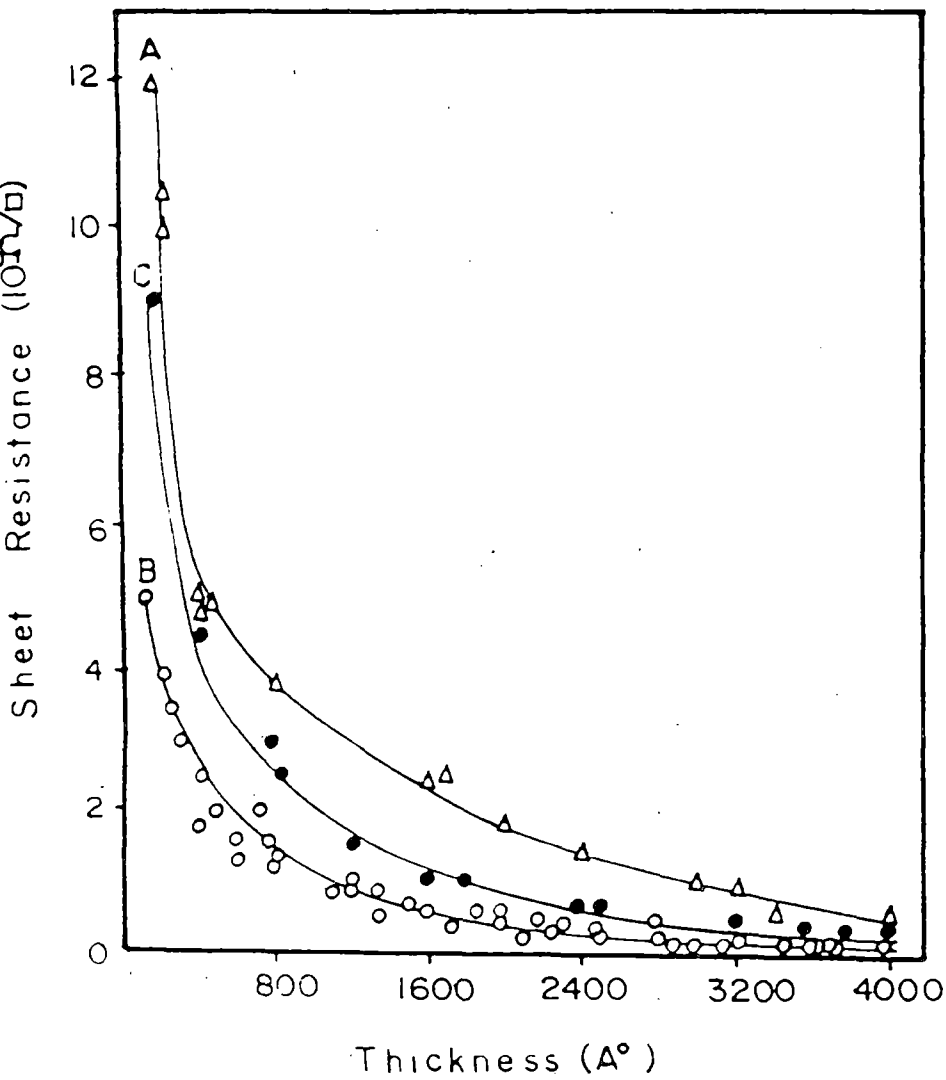

Figure 4.5. Variation of sheet resistance with thickness of undoped SnO_2 thin films deposited at various substrate temperatures. A, 350° C; B, 400° C; C, 450° C.

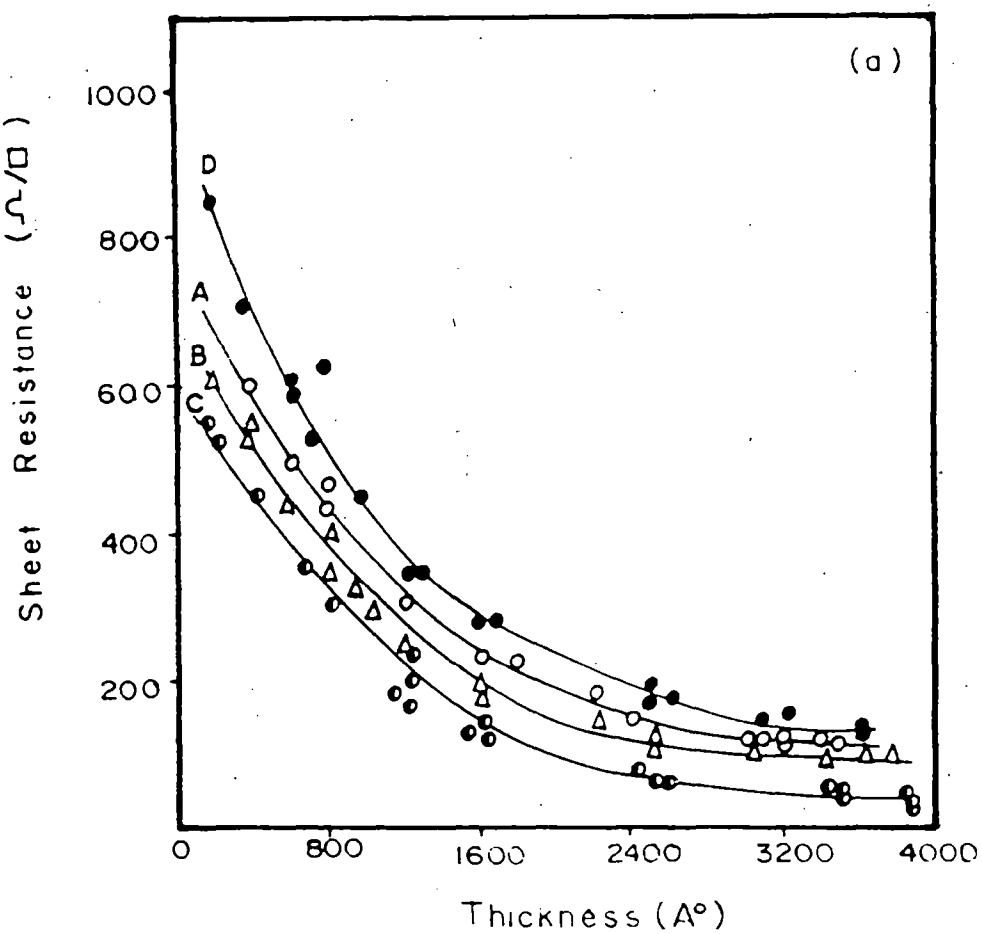

Figure 4.6. Variation of sheet resistance with thickness of doped SnO_2 thin films (T_s = 400° C), (a) Mo-doped SnO_2: A, 4 at%; B, 5 at%; C, 6 at% D, 7 at%.

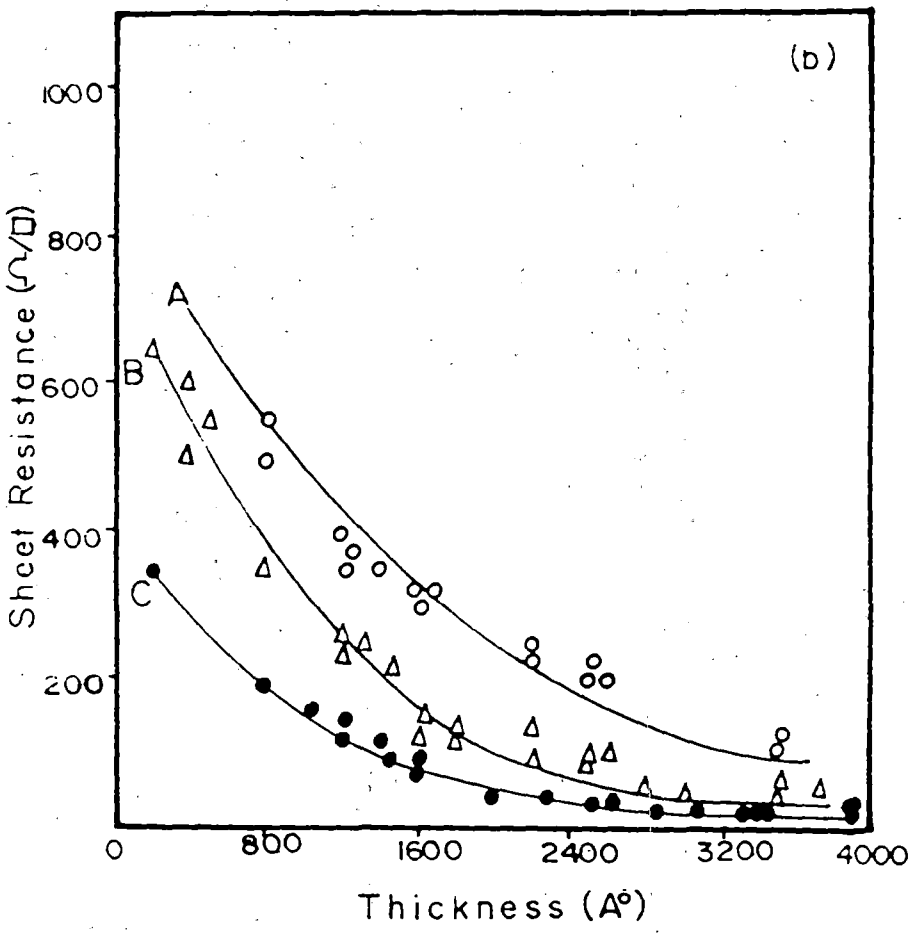

Figure 4.6. Variation of sheet resistance with thickness of doped SnO_2 thin films (T_s = 400° C), (b) Sb-doped SnO_2: A, 0.5 at%; B, 1.0 at%; C, 1.5 at%.

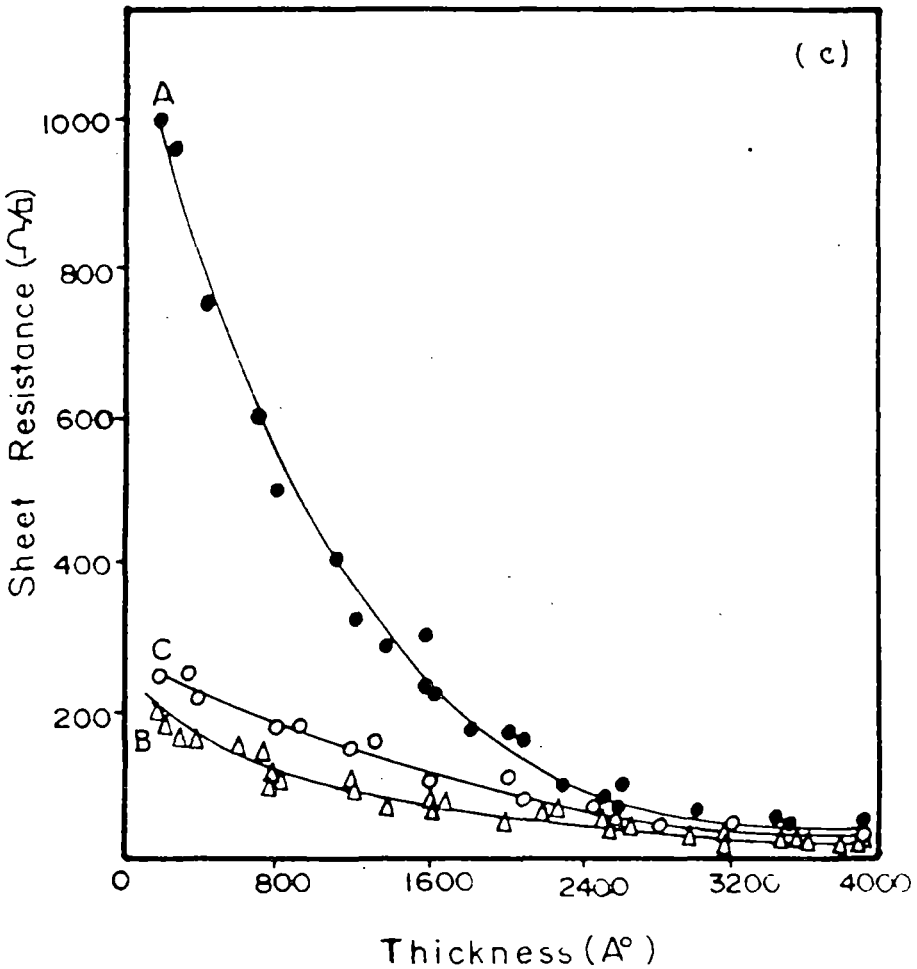

Figure 4.6. Variation of sheet resistance with thickness of doped SnO_2 thin films (T_s = 400° C), (c) F-doped SnO_2: A, 4 at%; B, 4.5 at%; C, 5 at%.

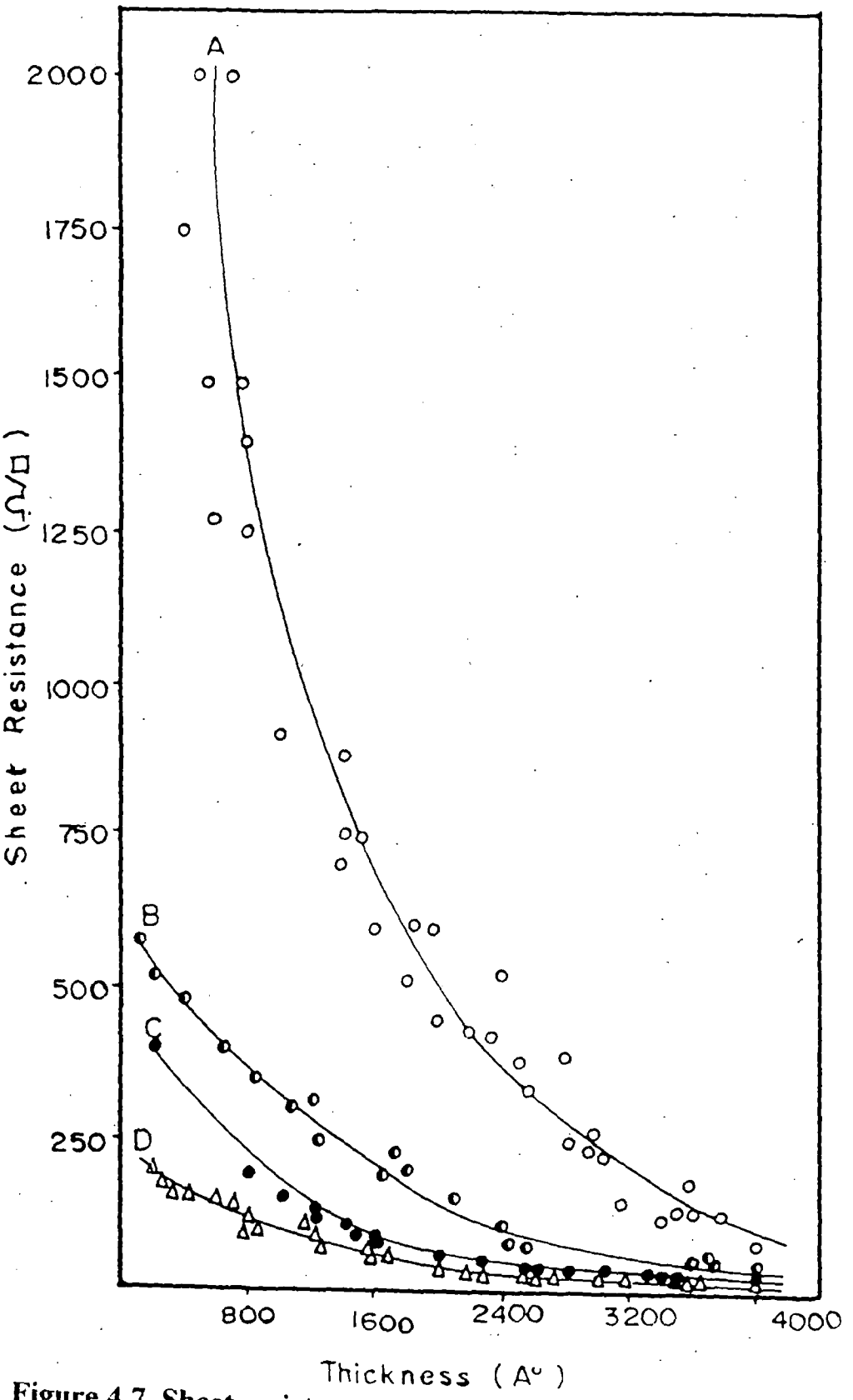

Figure 4.7. Sheet resistance versus thickness relationship for undoped [curvr A] and doped [curve B, SnO_2:Mo (6 at%); curve C, SnO_2:Sb (1.5 at%); curve D, SnO_2:F (4.5 at%)] SnO_2 thin films prepared at a substrate temperature of 400° C.

Effect of dopants [Mo, Sb & F] at various concentration on the resistivity is shown in figure 4.6. It is found that for every dopant, there is an optimum concentration at which the sheet resistance is a minimum. These values are listed in table 4.3.

Table 4.3. ***Minimum resistivity values of undoped and doped SnO_2 films on glass substrate (T_s = 400° C).***

Films	Resistivity (Ω cm.)
SnO2 (undoped)	4×10^{-3}
SnO2:Mo (6at%)	2×10^{-3}
SnO2:Sb (1.5at%)	8×10^{-4}
SnO2:F (4.5 at%)	4×10^{-4}

Thus it is observed that introduction of Mo reduces the resistivity by a maximum factor of two whereas Sb and F reduces it by a factor of five and ten respectively. Similar results are reported by G. Gordillo et al [46]. Relatively higher resistivity and lower optical transmission of the Mo-doped SnO_2 films compared to Sb-doped and F-doped films may due to their small grain size, as observed from the SEM micrograph. It is known that with decrease in grain size the grain boundary potential increase leading to increased grain boundary scattering and a corresponding increase in resistivity [12]. In the case of Sb-doped and F-doped SnO_2 films, the resistivity decreases upto 1.5 at% Sb doping and 4.5 at% F-doping respectively which may be due to (i) increased carrier concentration, (ii) larger grain size and (iii) preferred orientation. Beyond the above concentration the observed increase in resistivity may be due to the increase in contribution from ionised impurity scattering [21].

Variation of sheet resistance with thickness for optimum concentration of the dopants is shown in figure 4.7.

4.4.4. Optical Properties

The high optical transparency of these films in the visible and near IR regions of the solar spectrum in a direct consequence of SnO_2 being a wide bandgap semiconductor ($E_g \geq 3$ eV). The transmission in this region is limited by several factors [11]: (i) reflection losses which include both specular and scattered (diffuse) components (this backward scattering (about 1% - 2%) is primary due to surface roughness and increases with increasing thickness); (ii) absorption (about 1% - 2%) in the films, which is primarily due to free carriers; (iii) Variations in transmittance that may occur due to interference phenomena depending on the thickness of the film with the result that an average visible transmission must be described. The transmitted part of the incident energy also has specular and scattered (diffuse) components. This forward scattering (about 5%) is due to inhomogeneities in the film in the form of unreacted or partly reacted chemical species generated during the complex pyrolytic process, trapped gases, segregated impurity atoms of other oxide phases. Optical transmission as a function of wavelength in the range 400 nm to 800 nm was obtained by SHIMADZU UV - 240 double beam spectrophotometer.

The results for undoped and variously doped films for constant thickness and different sheet resistance values are shown in figure 3.8a, 3.8b, 3.8c and 3.8d. The optical transmission is observed to decrease with decreasing sheet resistance in case of both undoped and doped films. Variation of the average optical transmission as a function of sheet resistance for undoped and doped films are shown in figure 3.9. It is seen for all the films that the optical transmission drops off more rapidly at lower values of the sheet resistance. This is due to an increase in surface roughness of films having low sheet resistance which have a proportionately higher thickness. However, F-doped films are found to have high optical transmission even at a low resistivity of 4 X 10^{-4} Ω cm.

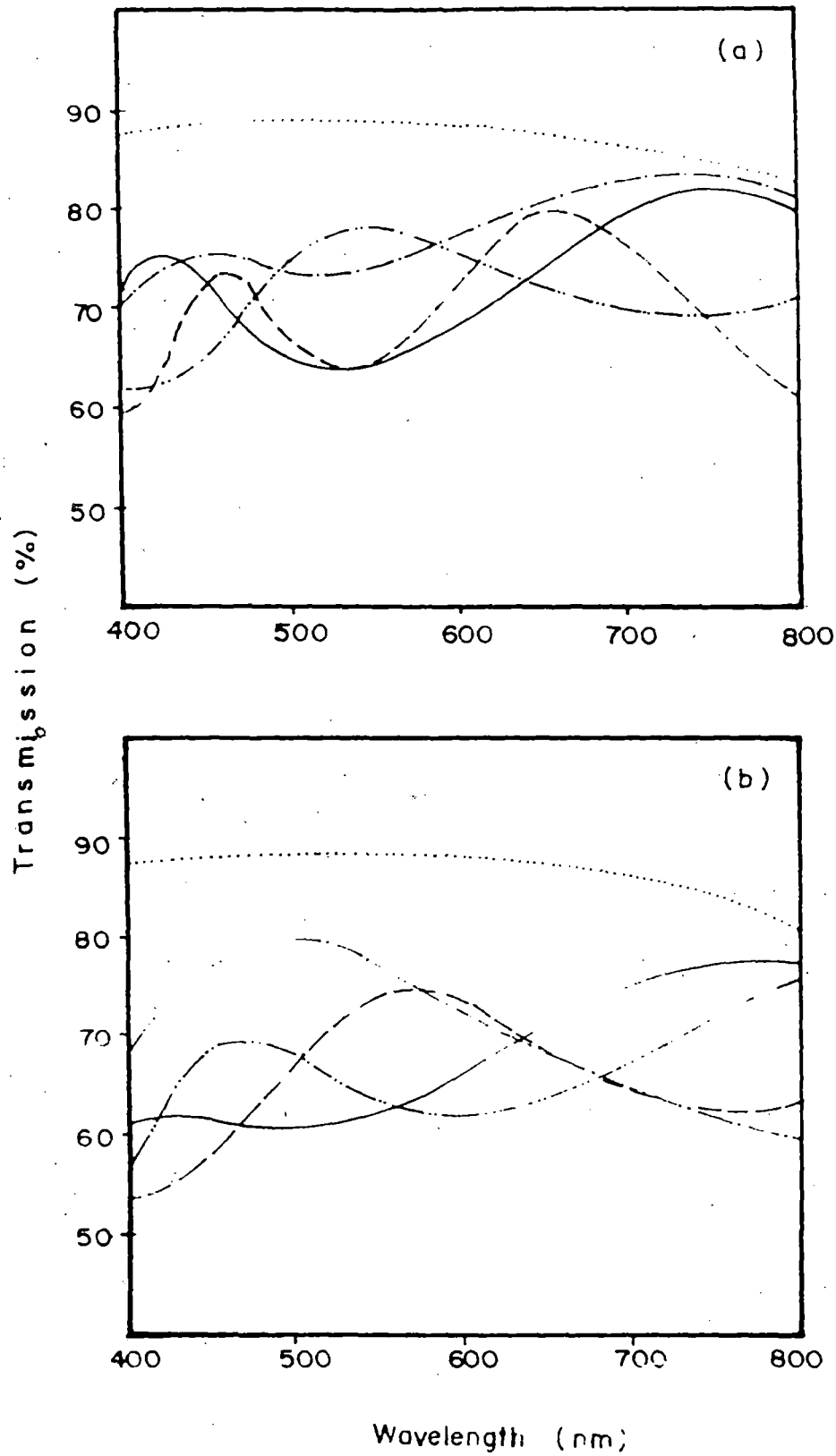

Figure 4.8. Optical transmission versus wavelength for typical SnO_2 thin films of various sheet resistance.(a) Undoped: (.....), bare substrate; (-.-.-.-) 700 Ω/□;(-..-..-..-) 400 Ω/□; (——) 350 Ω/□;(_____),200Ω/□. (b) Mo-doped (6 at%): (.....) bare substrate;(-.-.-.-) 525 Ω/□; (-..-..-..-) 200 Ω/□; (_____) 150 Ω/□; (——) 60 Ω/□.

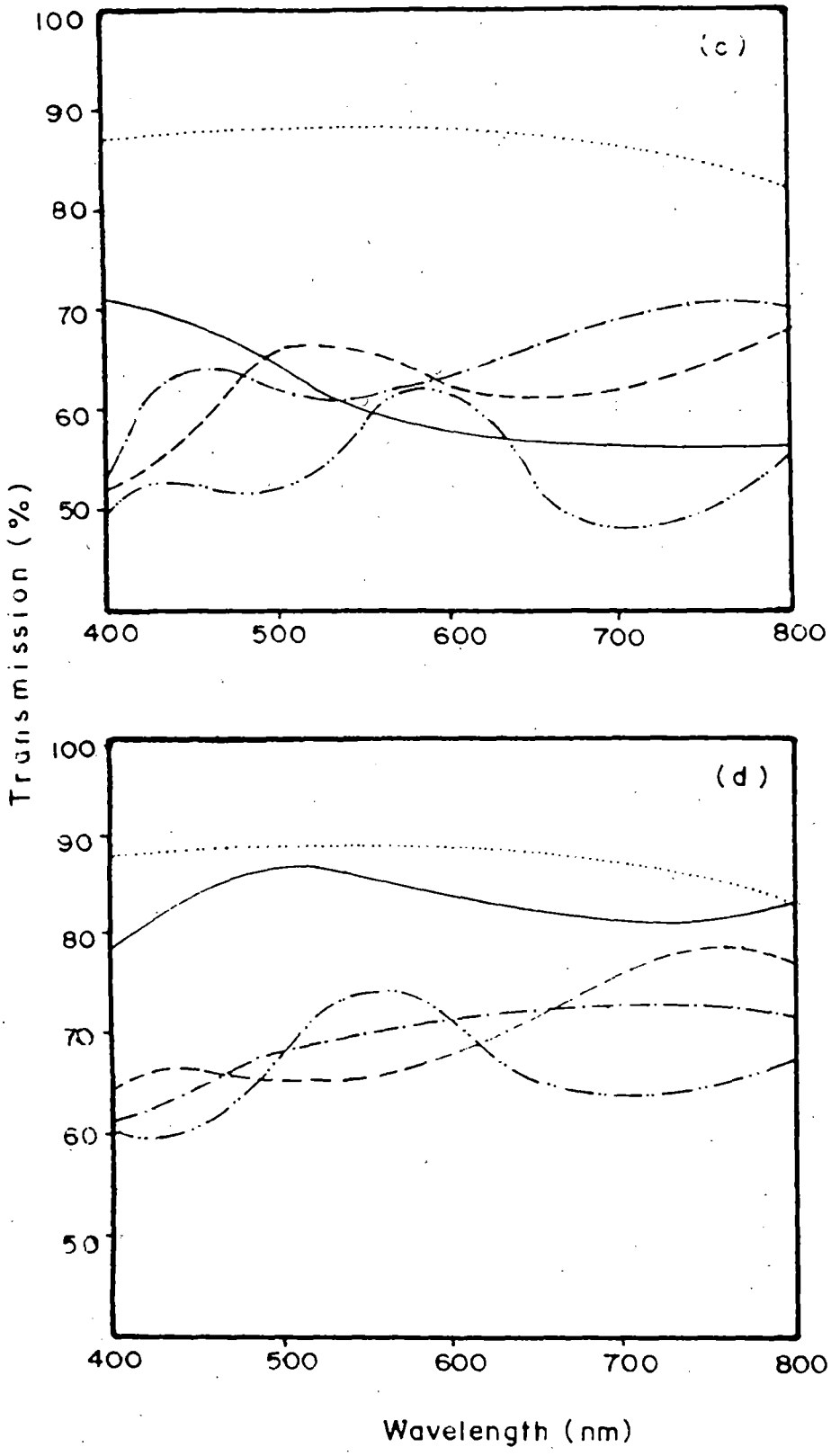

Figure 4.8. Optical transmission versus wavelength for typical SnO_2 thin films of various sheet resistance.(c) Sb-doped (1.5 at%): (.....) bare substrate; (_____)350 Ω/□; (——) 200 Ω/□; (-.-.-.-) 130 Ω/□; (-..-..-..-) 30 Ω/□.(d) F-doped (4.5 at%) : (.....), bare substrate; (_____) 160 Ω/□; (——) 90 Ω/□; (-.-.-.-), 60 Ω/□; (-..-..-..-) 20Ω/□.

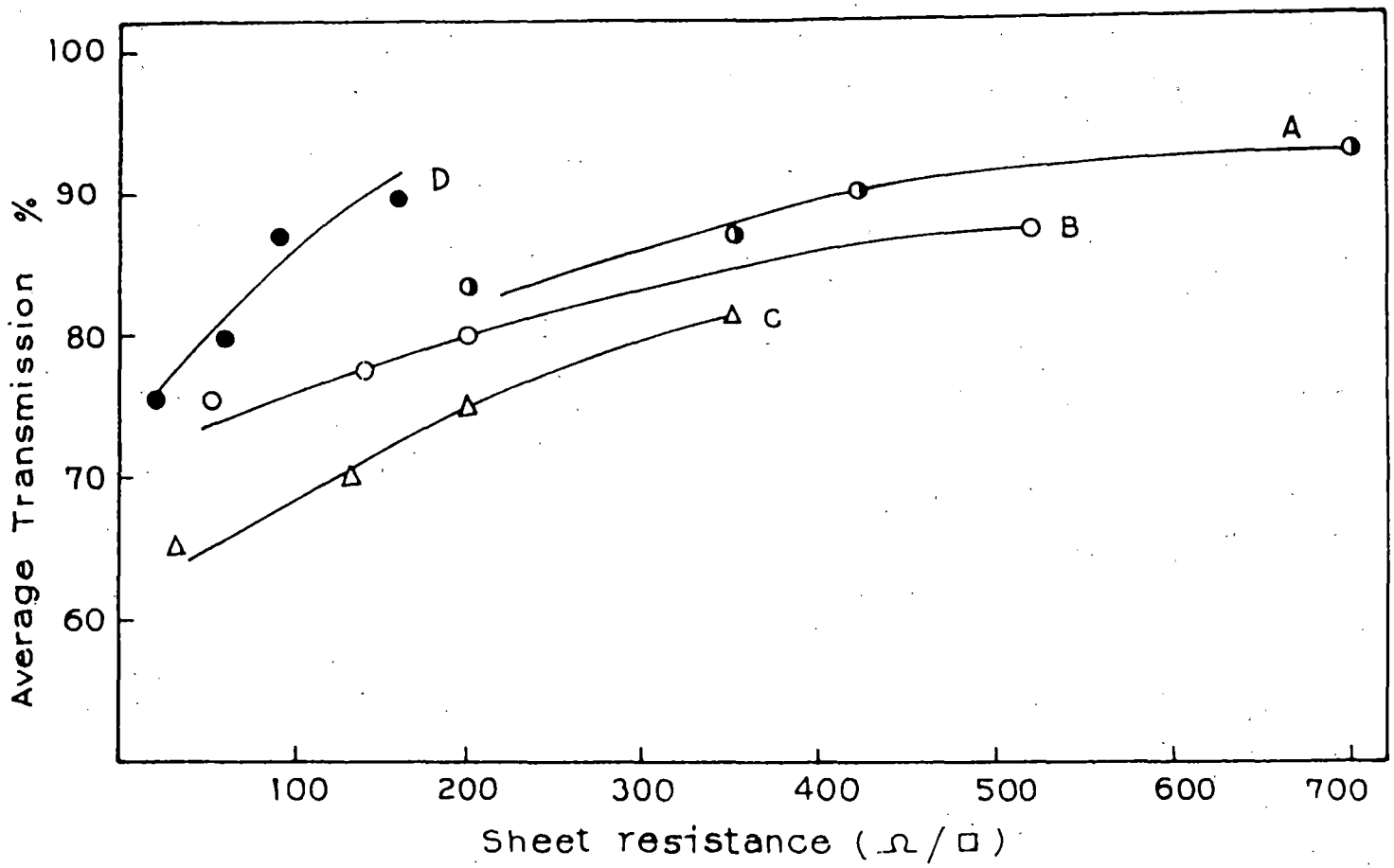

Figure 4.9. Average optical transmission over the range 400 nm - 800 nm versus sheet resistance for undoped [curve A] and doped [curve B, SnO_2:Mo (6 at%); curve C, SnO_2:Sb (1.5 at%); curve D, SnO_2:F (4.5 at%)] SnO_2 thin films prepared at a substrate temperature of 400° C.

4.4.5. Figure of merit

A figure of merit for transparent materials has been defined by the relation $\Phi_{TC} = T^{10}/R_S$ [38], where T is the optical transmission and R_S is the electrical sheet resistance. It is a useful tool for comparing the performance of transparent conductive coating when their electrical sheet resistance and optical transmission are known. Furthermore, the expression derived for Φ_{TC} can be used to predict the transparent electrode properties of a candidate material from its fundamental properties. The figure of merit is calculated for undoped and Mo, Sb and F doped SnO_2 films deposited by this method and compared with other workers. The calculated value and the results of other workers are tabulated in table 4.4.

4.4.6. Comparision of Electrical and Optical properties of tin dioxide films prepared by various workers.

The films are found to compare quite favourably in terms of electrical and optical properties with those prepared by other methods as shown in table 4.4 given below.

Table - 4.4. *Comparison of the electrical and optical properties of tin dioxide films prepared by various workers.*

Material	Deposition technique	ρ (Ω cm.)	R_S (Ω/□)	T (λ_r) % (μm)	ϕ_{TC} ($10^{-3}cm^{-1}$)
SnO_2	Spray pyrolysis [1]	5×10^{-3}	84	85 (0.5-2)	2.4
	CVD [54]	7×10^{-2}	1200	93 (0.3-0.7)	0.41
	Present work	4 x 10-3	100	90 (0.4-0.8)	3.48
SnO_2 :Sb	Spray pyrolysis [11]	4.2×10^{-3}	28	87 (0.3-1)	9.4
	CVD [20]	2×10^{-3}	55	88 (0.4-0.7)	5.06
	Present work	8×10^{-4}	20	75 (0.4-0.8)	2.82
SnO_2:F	Spray pyrolysis [11]	4.6×10^{-4}	10	85 (0.4-10)	19.68
	CVD [55]	5×10^{-4}	20	90 (0.4-0.8)	17.43
	Present work	4×10^{-4}	10	85 (0.4-0.8)	19.68
SnO_2:Mo	Present work	2×10^{-3}	50	70 (0.4-0.8)	2.15

ρ - Resistivity, R_S - Sheet resistance, T (λ_r) - Average optical Transmission (Wavelength), ϕ_{TC} - Figure of merit, **CVD** - chemical vapour deposition.

4.5. CONCLUSION

Undoped and Mo-, Sb- and F-doped tin oxide films of reproducible quality have been deposited by the Open Air Chemical Vapour Deposition (OACVD) technique. The films were smooth, highly uniform and resistant to peeling - off and acids, and also showed a high degree of crystallinity along with long term stability with respect to their optical, electrical and mechanical properties. X-ray diffractometric study suggests that Sb and F-doped SnO_2 films show preferred orientation along the (110) plane. Surface morphology study by scanning electron microscope suggests that for films deposited on glass substrates, the grain size increases in the case of Sb-doped and F-doped SnO_2 films but decreases for Mo-doped SnO_2 films when compared to undoped films. The grain size for undoped films on mica and aluminium sheet substrate is also larger than that for films deposited on glass substrates.

The lowest values of sheet resistance at a particular thickness are obtained for 6 at% Mo-doped, 1.5 at% Sb-doped and 4.5 at% F-doped SnO_2 films on glass substrate. A typical value of resistivity of 4.5 at% F-doped SnO_2 films is 4×10^{-4} Ω cm and that for 1.5 at% Sb-doped SnO_2 is 8×10^{-4} Ω cm.

The films compare quite well in terms of electrical conductivity and optical transmission with those obtained by other methods. The average optical transmission is found to decrease as the sheet resistance decreases for Mo and Sb-doped films. But for F-doped films, negligible increase in transmission loss with decrease in sheet resistance is found to occur.

Transparent conductors will continue to play an increasingly important role in electronic and opto-electronic devices. Further efforts are required to introduce such dopants and develop new processing techniques to satisfy the twin conflicting requirements of high optical transmission along with low resistivity. This is a totally unexplored area.

In conclusion, tin oxide films having a sheet resistance of 10 - 100 Ω Square^{-1} and an average optical transmission of 75% - 90% could routinely be obtained by this method. The merit of this method is its extreme simplicity by which one can deposit useful tin oxide films for device applications either on one side or both sides of a planar substrate or inside of a tube quite easily in any laboratory without using any specialized experimental set up. It is believed that using this method, ZnO, CuO, CdO, $CdSnO_2$ etc. oxide thin films also can be prepared.

REFERENCES

1. J. C. Manifacier, L. Dzepessy, J. F. Bresse and M. Perotin 1979 *Mater. Res. Bull.* **14** 163 (123)

2.W. Spence 1967 J. *Appl. Phys.* **38** 3767

3.Yar-Sun Hsu and Sorab K. Gandhi 1980 *II J. Electrochem. Soc., Solid State Sci. Technol.* **127** 1592

4. J. Bruneaux, H. Cachet, M. Froment, J. Amblard, J. Belloni and M. Mostafavi 1987 **Electrochem. Acta 32** 1533

5. J. Bruneaux, H. Cachet, M. Froment, J. Amblard, J. Belloni and M. Mostafavi 1989 *J. Electroanal chem.* **269** 375

6. P. Cowache, D. Lincot and J. Vedel 1989 *J. Electrochem. Soc.* **136** 1646

7. W. Badway, F. Decker and K. Doblhoffer 1983 *Solar Energy Mater.* **8** 363

8. J. C. Manifacier, J. P. Fillard and J. M. Bind 1981 *Thin Solid Films* **77** 67

9. B. Drevillon, K. Satytendra, P. Rocai Cabarrocas and J M. Siffert 1989 *Appl. Phys. Lett.* **54** 2088

10. P. Grosse, F. J. Schmitte, G. Frank and H. Kostlin 1982 *Thin Solid Films* **90** 309

11. K. L. Chopra, S. Major and D. K. Pandya 1983 *Thin Solid Films* **102** 1-46

12. C. S. Rastomjee, R. S. Dale, R. J. Schaffer, F. H. Jones, R. G. Egdell, G. C. Georgiadis, M. J. Lee, T. J. Tate & L. L. Cao 1996 *Thin Solid Films* **279** 98

13. Ireneusz Kocemba, Tadeusz Paryjczak 1996 *Thin Solid Films 272* 15

14. J. Kane, H.P. Schweizer and W. Kern 1976 *J. Electrochem. Soc.* **123** 270

15. B. J. Baliga and S. K. Gandhi 1976 *J. electroche. Soc.* **123** 941

16. M. R. Kadam, N. Vittal, R. N. Karckar and R. C. Aiyer 1990 *Thin Solid Films* **187** 199

17. T. P. Chow, M. Ghezzo and B. J. Baliga 1982 *J. Eletrochem. Soc.* **129** 1040

18. J. P. Upadhyay, S. R. Vishwakarma and H. C. Prasad 1989 *Thin Solid Films* **169** 195

19. A. Rohatgi, T. R. Viverito and L. H. Slack 1974 *J. Am. Ceram. Soc.* **57** 57

20. H. Kim and H. A. Laitinen 1975 *J. Am. Ceram. Soc.* **58** 23

21. E. Shanthi, A. Banerjee, V. Dutta and K. L. Chopra 1980 *J. Appl. Phys.* **51** 6243

22. E. Shanthi, A. Banerjee, V. Dutta and K. L. Chopra 1980 *J. Appl. Phys.* **53** 1615

23. U. R. Chaudhuri, K. Ramkumar and M. Satyan 1990 *J. Phys. D: Appl. Phys.* **23** 994

24. H. Watanabe,1970 *Jpn. J. Appl. Phys.* **9** 1551

25. T. Matsuoka, J. Kuwatov, M. Nishikawa, Y. Fujita, T. tohda and A. Abe 1988 *Jpn. J. Appl. Phys.* **27** 1088

26. H. W. Lehmann and R. Widmer 1975 *Thin Solid Films* **27** 359

27. J. L. Vossen and E. S. Polimiak 1972 T*hin Solid FIlms* **13** 281

28. A. Czapla, E. Kusior and M. Bucko 1989 *Thin Solid Films* **182** 15

29. J. P. Chatelon, C. Terrier, E. Bernstein, R. Berjoan and J. A. Roger 1994 *Thin Solid Films* **247** 162

30. C. Terrier, J. P. Chatelon, R. Berjoan and J. A. Roger 1995 *Thin Solid Films* **263** 37

31. C. J. Brinker, A. J. Hurd, P. R. Schunk, G. C. Frye and C. S. Ashley 1992 *J. Non-Crystalline Solids* **147 & 148** 424

32. Y. Takahashi and Y. Wada 1990 *J. Electrochem. Soc.* **137** 267

33. D. E. Carlson 1975 *J. Electrochem. Soc.* **122** 1334

34. T. Muranoi and M. Furukoshi 1978 *Thin Solid Films* **48** 309.

35. R. N. Ghoshtagore 1978 *J. Electrochem. Soc.* **125** 110.

36. G. N. Advani, A. G. Jordan, C. H. F. Luges and R. N. Longini 1979 *Thin Solid Films* **62** 361.

37. R. Kalbskopf 1984 *Thin Solid Films* **22** 65.

38. O. Tabata, T. Tanaka, M. Waseca and K. Kumhara 1979 *Surface Sci.* **86** 230.

39. K. B. Sundaram and G.K. Bhagver 1981 *Thin Solid Films* **78** 35.

40. J. A. Aboaf, V. C. Marcotte and N. R. Cronel 1973 *Electrochem Soc.* **120** 701.

41.M. K. Karanjai and D. DasGupta 1988 *J. Phys. D: Appl. Phys.* **21** 356.

42. H. Dislich and E. Hvssmann 1981 *Thin Solid Films* **77** 129.

43. Vossen J. L. 1977 Physics of thin films Vol. 9 ed. G. Hass, M. H. Francombe and R. W. Hoffmann (New York: Academic) P. 1-71.

44. A. L. Unaogu and C. E. Okeke, 1990 *Solar Energy Materials* **20** 29

45. A. De and S. Ray 1991 *J. Phys. D: Appl. Phys.* **24** 719

46. G. Gordillo, L. C. Moreno, W. de la Cruz, P. Teheran 1994 *Thin Solid Films* **252** 61

47. G. Haacke 1976 *J. Appl. Phys.* **47** 4086

48. J. Kane, H. P Schweizer and W. Kern 1975 *J Electrochemcal Soc.* **122** 1144

49. James Proscia and Roy G. Gordon 1992 *Thin Solid Films* **214** 175